Chapter

Photo-Detectors Based on Two Dimensional Materials

Mubashir A. Kharadi, Gul Faroz A. Malik and Farooq A. Khanday

Abstract

2D materials like transition metal dichalcogenides, black phosphorous, silicene, graphene are at the forefront of being the most potent 2D materials for optoelectronic applications because of their exceptional properties. Several application-specific photodetectors based on 2D materials have been designed and manufactured due to a wide range and layer-dependent bandgaps. Different 2D materials stacked together give rise to many surprising electronic and optoelectronic phenomena of the junctions based on 2D materials. This has resulted in a lot of popularity of 2D heterostructures as compared to the original 2D materials. This chapter presents the progress of optoelectronic devices (photodetectors) based on 2D materials and their heterostructures.

Keywords: 2D materials, graphene, silicene, TMDCs, responsivity, detectivity, photo-conductive gain

1. Introduction

Photodetectors are devices that sense the light and convert it into an electric current. Photodetectors are essential components of many devices that are a part of our day to day life [1–5]. Primarily, silicon (Si) has been a material of choice for photodetector applications. Such photodetectors are readily integrated with complementary metal oxide semiconductor (CMOS) technology. The aggressive scaling has reduced the cost of Si-based devices and expanded their range of applications. Though Si photodetectors have evolved and developed over the years. But their performance is limited by the indirect nature of the bandgap of Si. The absorption of Si is limited to the visible and near-infrared parts of the electromagnetic spectrum. Also, the indirect nature of Si's bandgap leads to phonon generation to conserve the momentum during the light assisted transition of carriers from lower energy to higher energy. These phonons lead to scattering of the carriers and thereby reduce the efficiency of Si photodetectors. Also, Si as a material is not a good absorber of light in bulk form, further degrading Si photodetectors' efficiency. These limitations of Si photodetectors have prompted a quest in the research community for alternate materials. Two dimensional (2D) materials, among the class of novel materials for optoelectronic applications, have shown favorable characteristics. Features like direct nature and wide range of bandgap, atomically thin nature, efficient light-matter interaction, and heterostructures forming are interesting. The class of 2D materials encompasses materials like graphene,

transition metal-di-chalcogenides (TMDCs), Xenes etc. 2d materials are artificially derived materials. These materials are derived from layered van der Waals solids. In van der Waals solids, the atomic arrangement is such that the constituent atoms are held together by covalent or ionic bonds giving rise to atomic layers, whereas these atomic layers are held together by van der Waals interactions. The weak nature of van der Waals forces makes it possible to cleave individual layers from these materials. It is possible to obtain a free-standing single atomic or few atomic layers via mechanical exfoliation [6, 7] or liquid phase exfoliation [8, 9]. Graphene, which is a single layer of carbon atoms arranged in a hexagonal manner, is regarded as the original 2D material. Over the years, it has been revealed that graphene possesses many appealing electronic, mechanical, optical and thermal properties. [10–12]. Interaction of light with graphene occurs over a broad bandwidth range (terahertz to ultraviolet wavelengths) because of semi-metallic/gapless nature. This makes graphene a candidate for wide spectral range photodetectors. The atomically thin nature of graphene limits its absorption coefficient [13–15]. Graphene absorbs only 2.3% of incident light (visible and ultraviolet), making this a primary limitation of graphene for photodetector applications. A high absorption coefficient is desirable for an optimum magnitude of photocurrent [16–18]. For the efficient operation of a photodetector, a longer lifetime of the photo exited carriers is desired. Graphene's gapless nature results in a shortened lifetime of photo-excited carriers, which further limits graphene photodetectors' performance. Beyond graphene, TMDCs have also attracted a lot of attention for optoelectronic applications over the past decade. One advantage of TMDCs over graphene is their semiconducting nature. TMDCs possess varied bandgaps, thus making them applicable for broadband photodetection. TMDCs can be represented by the general formula of MX2, where M represents a transition metal and X represents a chalcogenide atom. The arrangement of atoms in MX2 is such that the metal atom is sandwiched between the two chalcogenide atoms, as shown in **Figure 1**. TMDCs detect light at different wavelengths because of layer dependent bandgap [19–21]. Most of the TMDCs have a direct

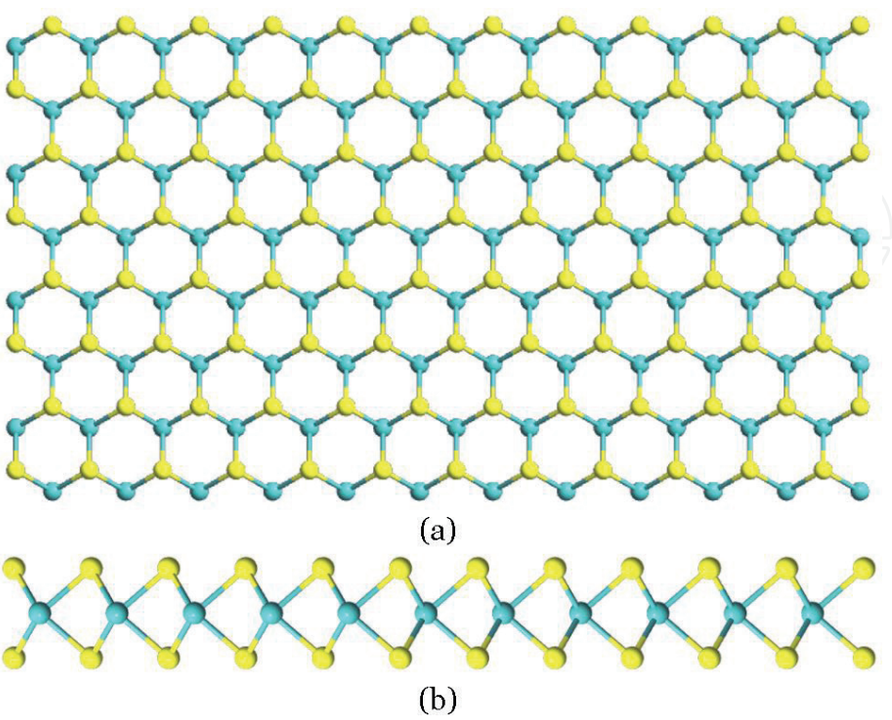

Figure 1.
Structural arrangement of TMDCs (MoS_2). (a) Top view and (b) side view. Cyan and Yellow balls are Molybdenum and Sulfur atoms respectively.

nature of the bandgap, limiting the phonon scattering in TMDCs photodetectors, which leads to better efficiency [22]. 2D materials have localized electronic bands, leading to sharp peaks in the density of states (DOS) called Van Hove singularities at specific energies [22]. Generally, in 2D materials like TMDCs, these singularities reside near conduction and valence bands. This leads to an increased probability of electron–hole pair generation upon excitation with light [22, 23]. TMDCs photodetectors show excellent light to current conversion with high responsivity [22]. Although TMDCs based photodetectors have shown an appealing development in their performance over the years, these devices are limited by slow response speed. Furthermore, TMDCs photodetectors are still behind the absorption efficiency of bulk Si photodetectors. Apart from these 2D materials, materials like silicene, phosphorene etc., have shown promising theoretical results as far as optoelectronic applications are considered.

Though the field of 2D materials is still developing, the early results of optoelectronic devices based on these materials are very promising. The unique properties of 2D materials have ushered in a lot of theoretical and experimental research for optoelectronic applications over the past decade or so. This has led to the proposal of numerous photodetectors based on 2D materials both theoretically and experimentally. This chapter aims at presenting an insight into the novel photodetectors based on 2D materials. Section 2 offers a discussion on photodetectionchanisms in 2D materials. Section 3 presents a discussion on photodetectors based on 2D materials and their heterostructures; Section 4 presents a brief summary of the chapter and future scope of 2D materials for photodetector applications.

2. Photodetection mechanisms in 2D materials

Generally, photocurrent generation mechanisms are divided into three categories, viz. photovoltaic effect, photo-thermoelectric effect, and photo-bolometric effect. In the photovoltaic effect, a built-in electric field results in the separation of the electrons and holes. This built-in electric field may be generated due to a Schottky barrier at the metal–semiconductor interface. Photodetectors working under this mechanism are called photodiodes. In the photo-thermoelectric effect, a non-uniform light source is used. This light source leads to non-uniform heating of the channel, resulting in a temperature gradient within the channel. Due to this temperature gradient, carriers move from the high-temperature region to the low-temperature region. The migration of the carriers leads to their accumulation in the low-temperature region, which results in a potential. The photo-bolometric effect is based on uniform heating of the material under illumination. This uniform heating results in a change in the resistivity of the material. This effect is directly proportional to the variation of the material's conductivity and the increment in temperature caused by light irradiation. In contrast to the photo-thermoelectric effect, the photo-bolometric effect does not drive the current but only changes the intensity of the current under external bias and illumination.Another unique mechanism observed in optoelectronic devices like photodetectors is internal photoemission (IPE). IPE involves photoinjection of electrons from an emitter/source (metal or semiconductor) into the conduction band of a collector/drain (semiconductor or insulator) in a BJT/FET. The holes are photoinjected into the valence band of the collector/drain and is called as hole photoemission [24]. In IPE, an optical excitation of electrons in the metal to an energy above the Schottky barrier is involved. These excited electrons are then transported to the conduction band of the semiconductor. The Initial theory of IPE was proposed by Fowler [25, 26]. However, this theory does not take the thickness of the Schottky

metal layer into consideration. Over the years the original theory of IPE has been refined largely resulting in much better assessment of the performance of the devices based on this effect [27, 28].

3. Photodetectors based on 2D materials

3.1 Graphene photodetectors

Graphene is regarded as the original 2D material and has a hexagonal arrangement of atoms. Graphene has a planar geometry contrary to some other 2D materials like Xenes (silicene, germanene stanene etc.). The Xenes, in general, have a buckled geometry wherein the two sub lattices of the hexagonal lattice are slightly displaced with respect to each other. Graphene can absorb light with a wavelength ranging from ultraviolet to mid-infrared [29, 30]. Graphene has small optical absorption due to its atomically thin nature, limiting the photoresponsivity of the photodetectors based on it. A graphene photodetector exhibited a bandwidth of 500 GHz and a photoresponsivity of 0.5 mAW^{-1} [31]. A metal-graphene-metal (MGM) photodetector having asymmetric electrodes has been investigated for extended operating frequency. This device shows an external photoresponsivity of 6.1 mAW^{-1}.

Some of the essential advantages of graphene photodetectors are high speed, ultra-broadband frequency range, and compatibility to circuits [32]. Compared to conventional semiconductors, graphene photodetectors show low photoresponsivity, which proves to be a significant drawback of such photodetectors. To overcome this and the other drawbacks, some techniques have been proposed to improve graphene photodetectors' optical absorption. For example, the use of nanostructured plasmonics leads to enhanced light concentration in the device via plasmonics resonance [33, 34]. This helps in improving the local electric field [33, 34]. Apart from enhancing the quantum efficiency, the plasmonics can also help in achieving multicolor detection [35]. A graphene photodetector possessing plasmonics nanoantennas sandwiched between two graphene layers shows a quantum efficiency of up to 20%. Though this method may offer quantum efficiency improvements, it reduces the device's operational bandwidth as the nanostructures' resonance determines the working wavelength in these systems.

Another method to improve graphene photodetectors' photoresponsivity is to integrate quantum dots with graphene [36]. The photoresponsivity and photodetection gain of such a device are 10^7 AW^{-1} and 10^8, respectively. The presence of quantum dots in this device helps the photo-excited carriers (electrons or holes) to reach the graphene sheet while trapping the opposite type of carriers (holes or electrons). This leads to a phenomenon known as field-effect doping. Graphene photodetectors using PbS quantum dots have also been fabricated [37]. The device portrays a photoresponsivity of 10^7 AW^{-1}. Graphene-quantum dot photodetectors are limited by factors like low operational speed and low operating bandwidth.

Another method to improve the photoresponse in graphene photodetectors is to use micro-cavities [38–42]. Such photodetectors are characterized by high speed, high efficiency, ultra-wide bandwidth and high photoresponsivity. The disadvantage of using micro-cavities is that the device's dimensions are relatively large compared to traditional photodetectors [41].

3.2 Molybdenum disulfide (MoS_2) photodetectors

MoS_2 in its monolayer form has exciting properties like high carrier mobility 200 cm^2V^{-1} s^{-1} [8, 43, 44], direct bandgap of ≈1.8 eV [43, 45], high On/Off ratio of

current [45], strong light-matter interaction [8, 44], mechanical flexibility, chemical stability and ease of processing etc. Such exciting features of MoS_2 in its monolayer and few-layer forms make it the most widely studied 2D semiconductor for optoelectronic applications. A photodetector having a typical field-effect transistor (FET) configuration was first reported by Yin et al. [46]. The device comprises of a mechanically exfoliated monolayer of MoS_2 monolayer nanosheet as the effective region. The device shows a unique response with a cut-off wavelength of 670 nm. The cut-off wavelength is consistent with the bandgap of MoS_2 in its monolayer form (1.8 eV). The maximum responsivity of this device is 7.5 mAW^{-1} along with a response speed of 50 ms. A similar photodetector/phototransistor was reported by Lopez-Sanchez et al. [47]. Again, this device is based on an exfoliated MoS_2 monolayer but has an improved responsivity of 800 mAW^{-1} and a cut-off wavelength of 680 nm [47]. The model of the device is shown in **Figure 2**. The improvement in the device performance is attributed to improved mobility of the carriers, quality of the contacts and positioning technique. Apart from improved responsivity, the device portrays a low noise equivalent power (NEP) of 1.5×10^{-15} $WHz^{-1/2}$. Such a low value of NEP is associated with a low value of dark current.

Furthermore, the dark current in this device is limited by the bandgap of MoS_2, which reduces the role of thermally excited carriers. However, the device is relatively slow in its response time, which is of the order of several seconds. Though the response time can be reduced (to 0.6 s) by using short pulses on the gate terminal to remove trapped charges, the response time is still considerable compared to other devices [46]. The photodetector reported by Lopez-Sanchez et al. shows a sub-linear dependence of photocurrent on the intensity of the light. Such behavior and the surrounding dependent response speed of MoS_2 indicate that charge trapping in MoS_2 and/or at the MoS_2-SiO_2 interface plays a vital role in the sensing process.

Some of the properties and qualities of MoS_2 depend on the number of layers; accordingly, the performance of the photodetectors varies with the number of layers of MoS_2 [43, 45, 48]. For example, in bulk form, MoS_2 is an indirect bandgap semiconductor and is not suitable for optoelectronic applications, whereas, in its monolayer form, it is a direct bandgap semiconductor, making it suitable for optoelectronic applications. The lifetime of the photoexcited carriers is also dependent on the number of layers. Lee et al. have fabricated phototransistors, having single, double and triple layer MoS_2 as the effective region. The optical bandgap of monolayer MoS_2 is 1.82 eV, whereas, for double and triple layer MoS_2, it is 1.65 eV and 1.35 eV, respectively. Based on the observations, it is seen that triple layer MoS_2 photodetector shows good detection for the red light, whereas double and monolayer MoS_2 photodetectors show good detection for the green light. The layer dependent bandgap in MoS_2 allows for its use in wavelength range up to near-infrared (NIR) [49]. Multilayer MoS_2

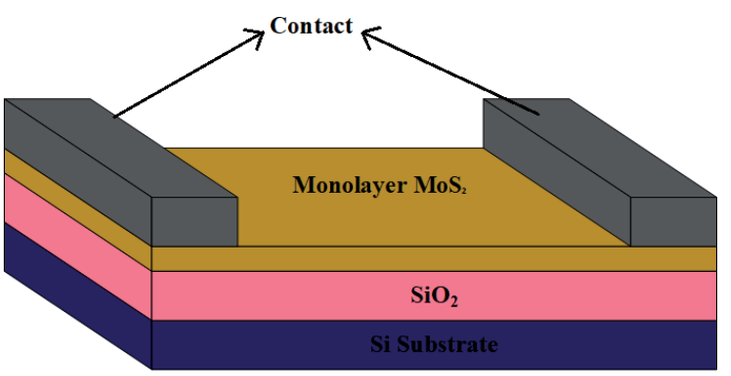

Figure 2.
Model of the exfoliated single layer MoS_2 phototransistor [47].

phototransistors show a degraded responsivity value of 100 mAW^{-1}. Khan et al. have also demonstrated that parameters like responsivity and response speed show a high dependence on the number of MoS_2 layers [50].

The properties of 2D MoS_2 are distinctly dependent on the method of preparation. Zheng et al. reported a phototransistor based on chemical vapor deposition (CVD) grown MoS_2 [51]. This device has a maximum responsivity of 2200 AW^{-1} in vacuum operating at a wavelength of 532 nm. The same device shows a responsivity of 780 AW^{-1} in air. The cause for such a decrease in responsivity is the adsorbates. Due to the large surface-to-volume ratio of MoS_2, many adsorbates migrate from ambient air to the surface of MoS_2 and the MoS_2/substrate interface. These adsorbents act as p-type dopants, leading to carrier scattering and degraded carrier mobility and responsivity in air. The photoresponse could also get affected (decreased) as the adsorbents may act as recombination centers for photoexcited carriers [52].

Perea-Lopez et al. have also fabricated a photodetector based on CVD-grown MoS_2 monolayer [53]. The reported device shows a relatively lower responsivity of 1.1 mAW^{-1} at an illuminating wavelength of 514.5 nm [53]. Such a considerable variation in the two devices' responsivity shows the significant role of contact resistance in these devices. Another study has put CVD-grown few-layer MoS_2 to use for a photodetector [54]. The performance of the device has been evaluated under harsh conditions with a wavelength of 532 nm [54]. Even at 200°C, the device portrays a photocurrent to dark current ratio of 10. Photodetectors based on MoS_2 employing other methods of synthesis like liquid exfoliation [55], solution synthesis [56] and magnetron sputtering [57] have also been reported. As compared to mechanically exfoliated and CVD grown MoS_2 based devices, these devices show degraded values of responsivities.

In photodetectors, based on monolayer and bilayer MoS_2, both photoconductive and photogating effects were observed to contribute to the photocurrent [58]. Different response times were observed for the two effects, respectively, making it possible to identify their independent contribution to the photocurrent. The photogating effect shows an obvious dependence on the gate voltage and is a slow process. The slowness of this effect comes from the longer lifetime of the trapped charges at the MoS_2-SiO_2 interface. In contrast, the photoconductive effect has a negligible dependence on the gate voltage and is a fast process. The fast response of the photoconductive effect arises from the mid-gap states due to structural defects in MoS_2. The photoconductive response can be studied independently by varying the illuminating light faster than the photo-gating effect.

In view of the average performance of MoS_2 photodetectors, several techniques have been proposed to improve their performance [59–66]. One such technique proposed by Leu et al. involves micro-patterning and localized modification of the MoS_2 layer [59]. The device is operated at an illuminating wavelength of 532 nm. The local modification is achieved by surface oxidation and oxygen doping. A photodetector based on such a modified MoS_2 layer shows improved photoresponse with a responsivity increase of several folds [59]. Kwon et al. proposed a photodetector based on multilayer MoS_2 with a bottom gate configuration [60]. As compared to previously reported global gate counterparts, the device shows much-improved photocurrent [49, 60, 67]. The purpose of a bottom gate in such a device is to impose a large tunnel barrier at ungated channel regions, which helps accumulate holes, thereby reducing the potential barrier for free electrons. Once the potential barrier is reduced, there is an increase in the electron depletion region's thermionic current. Furthermore, photocurrent improvement in the accumulation region arises due to decreased tunnel barrier for photoexcited holes. Also, the dark current is suppressed because of the series resistance from ungated areas.

Consequently, the responsivity shows huge improvements and attains a value of 342.6AW^{-1}. Kufer et al. fabricated a MoS_2 photodetector, wherein HfO_2 encapsulates the MoS_2 layer. Upon encapsulation, it was seen that the electronic and optoelectronic properties of multilayer MoS_2 photodetector improved [61]. The encapsulated MoS_2, along with negligible hysteresis in the transfer characteristics, showed an enhanced n-type behavior. Encapsulation decreases the number of surface adsorbents, which eventually leads to improved performance. Encapsulation results in an increase in the mobility of carriers and a decrease in the contact resistance. These two effects, in combination, give rise to an increased response speed and responsivity. The device's responsivity can be tuned by the gate voltage and ranges from 10 to 10^4 AW^{-1}.

3.3 Other TMDCs photodetectors

Apart from MoS_2, other TMDCs have been utilized for photodetector applications. These include $MoSe_2$, WS_2, WSe_2, $MoTe_2$, ReS_2 and $ReSe_2$. This section presents photodetectors based on these materials.

Like MoS_2, monolayer $MoSe_2$ has several alluring properties, such as a direct bandgap of 1.5 eV [68], enhanced photoluminescence (PL) [69] and considerable binding energy of excitons [70]. Improvements in the synthesis of $MoSe_2$ via mechanical exfoliation [71, 72] and CVD methods [73–75] have widened their scope of photodetector applications. Chang et al. and Xi et al. have reported monolayer $MoSe_2$ phototransistors [76, 77]. $MoSe_2$ monolayers for the phototransistors were prepared via CVD methods. The responsivities of the phototransistors are of the order of mAW^{-1}, which is lower than the CVD-grown MoS_2 monolayer counterparts by a few orders [51]. However, if the density of the charge impurities and defects are reduced, an improved photoresponse of the order of tens of milliseconds is expected. The responsivity of $MoSe_2$ based devices can be improved by using a CVD-grown multilayer $MoSe_2$ [78]. But the improvement comes at the cost of degraded response speed [78]. A phototransistor based on a few-layer $MoSe_2$ has been fabricated by Abderrehmane et al. [72]. $MoSe_2$ layers were obtained by mechanical exfoliation methods [72]. This device has a response time of tens of milliseconds and a responsivity of 97.1 AW^{-1} operating at a wavelength of 532 nm.

Photodetectors based on monolayer and few-layer WS_2 obtained via different synthesis methods have been reported [79, 80]. The photoresponse of CVD-grown few-layer WS_2 has been studied by Parea-Lopez et al. [81]. The photoresponse reportedly shows a high dependence on photon energy [81]. The responsivity and response speed of the device are reported to be 92 μAW^{-1} and 5 ms, respectively at a wavelength of 457-647 nm. The dependence of multilayer WS_2 devices' responsivity was observed to depend on the surrounding gaseous environment by Huo et al. [82]. The responsivity shows an increase when the environment changes from vacuum (tens of AW^{-1}) to NH_3 (884 AW^{-1}) at a wavelength of 633 nm. The increased responsivity is a consequence of the charge transfer between the NH_3 gas molecule and WS_2. The doping level of WS_2 gets modified by the charge transfer, which eventually increases the lifetime of photoexcited carriers and hence the responsivity. Another study conducted by Lan et al. showed a similar surrounding dependent performance of WS_2 devices [83]. The device showed a decrease in its responsivity from 18.8 mAW^{-1} in vacuum to 0.2 μAW^{-1} in air.

Monolayer and few-layer WSe_2 has also been studied for photodetector applications. Zheng et al. have fabricated photodetectors using CVD-grown WSe_2 monolayer [84]. The effect of metal contacts having different work functions on the device's photoresponse is studied [84]. The device exhibits the maximum (1.8 × 10 5 AW^{-1}) and minimum responsivity with Pd and Ti contacts at a wavelength of

650 nm. However, the device with Ti contacts shows a much smaller response time (23 ms) than the device with Pt contacts. The variation in the device's performance results from the considerable difference in Schottky barriers between WSe_2 and different materials, highlighting the significant role of metal contacts in these devices. Pradhan et al. have demonstrated a photodetector based on a trilayer WSe_2 [85]. The device exhibits the responsivity and response speed of $7AW^{-1}$ and 10 μs, respectively at an illuminating wavelength of 532 nm. Other reports involving graphene contacts and doping of a few-layer WSe_2 have been observed to improve the performance of WSe_2 photodetectors [66, 86, 87].

A newly introduced 2D material, $MoTe_2$ has excellent electronic and optoelectronic properties, due to which it has received a lot of attention recently [88–90]. Yin et al. have reported a phototransistor based on exfoliated few-layer $MoTe_2$ [91]. A study of the effect of different metal contacts on the electrical properties of the $MoTe_2$ phototransistor is presented. The device attains a responsivity of 2.56×10^3 under optimum conditions under an illumination of 473 nm laser.

Re-dichalcogenides are different from the majority of other layered TMDCs due to their high crystal symmetry. ReS_2 and $ReSe_2$, in their distorted 1 T in-plane structure are anisotropic semiconductors [92]. The electrical, mechanical, and optical properties of these materials are extremely anisotropic, rendering these materials interesting for optoelectronic and electronic applications. The bandgap and carrier mobility of $ReSe_2$ was found to be dependent on the layer thickness by Yang et al. [93]. This allows modification of the electronic and optoelectronic properties of ReS_2 devices. A monolayer $ReSe_2$ phototransistor has an exceptional photoresponse with responsivity and response time of 95 AW^{-1} and tens of milliseconds, respectively [93]. The operating wavelength for the device is chosen to be 633 nm. Just like MoS_2 and WS_2 devices, the photoresponse of $ReSe_2$ devices is also found to be dependent on the surroundings [50, 51, 82, 83, 94]. The charge transfer between the surrounding gas and $ReSe_2$ consequently affects the device performance. This charge transfer alters the doping in $ReSe_2$ along with the carrier lifetime [94]. One way to avoid this dependence of performance on surroundings is to use encapsulation or passivation. Though the $ReSe_2$ photodetectors/phototransistors show promising results but an obvious disadvantage of these devices is that the current after removing the illuminating light can not return to dark current levels. This disadvantage is a consequence of the slow recombination rate of the photoexcited carriers. However, this issue may be solved by applying short pulses at the gate terminal to reset the device [36].

Because of the anisotropic crystal structure, ReS_2, in particular, can be utilized to detect polarized light [95]. The model of one such photodetector is shown in **Figure 3**. The responsivity of ReS_2 photodetectors can be largely improved up to the levels of 3.97×10^3 to 1.18×10^6 by electron doping [96] under illumiation of a 1064 nm laser. Besides improved responsivity, the device portrays a broad range of wavelength detection and fast response speed of the order of tens of milliseconds. Significant enhancement in both the electronic and optoelectronic properties of ReS_2 via O_2 plasma treatment was observed by Shin et al. [97]. The device exhibits a high responsivity of 2.5×10^7 AW^{-1} at a laser illumination of 405 nm, which is the highest obtained for a 2D semiconductor based back gated photodetector. Such a high responsivity is a consequence of large thickness (30 nm) and direct bandgap of ReS_2 layers. The response time is observed to be inversely proportional to the plasma treatment duration. Prolonged plasma treatment leads to the formation of trap states within the bandgap of ReS_2. Such trap states result in enhanced recombination rates of photoexcited carriers, which consequently reduce the response time.

In summary, TMDCs photodetectors/phototransistors show a widely varying performance. Responsivities and the response times range from 10^{-7} AW^{-1} to 10^7

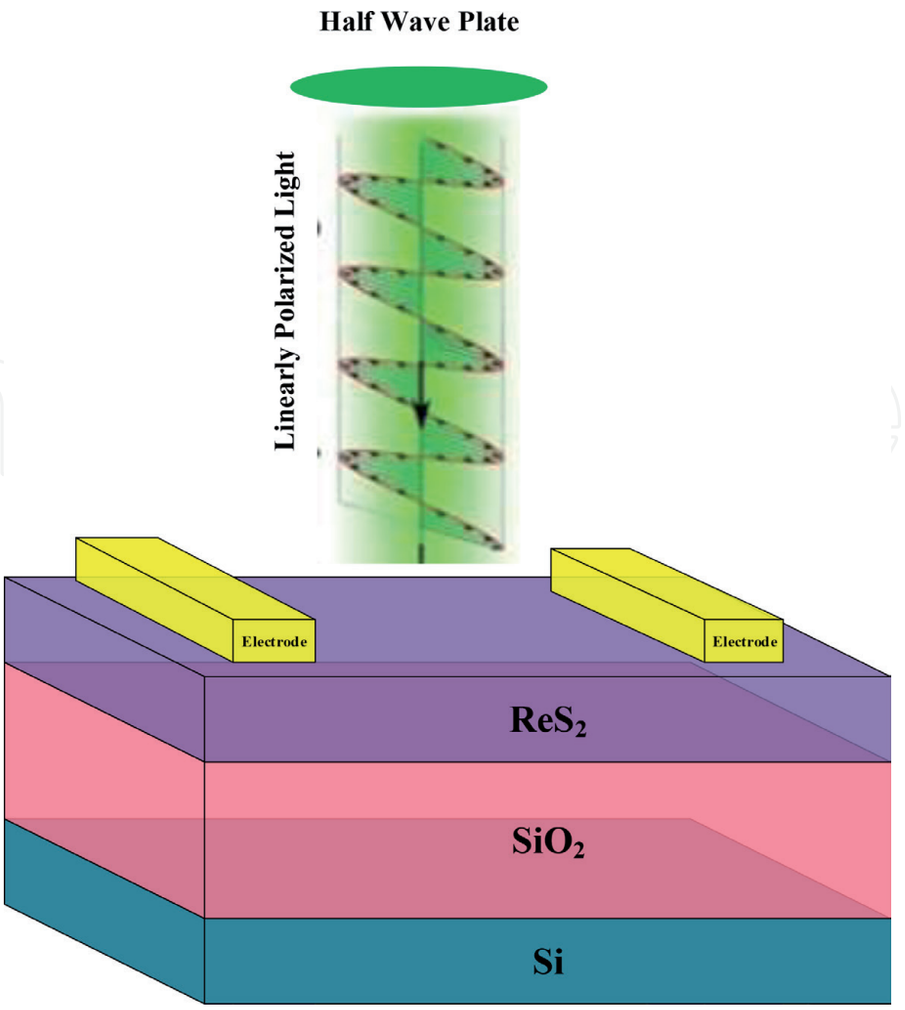

Figure 3.
Model of ReS_2 photodetector [95].

and 10^{-5} to 10^{3}, respectively. Generally, trap states affect the performance of TMDCs photodetectors. An increase in responsivities is observed at the existence of the trap states in TMDCs and/or at TMDC-dielectric interfaces. However, the response speed is found to decrease because of these trap states. Other factors that affect the TMDCs photodetectors/phototransistors are synthesis methods, number of layers, contact resistance and surrounding environment.

3.4 Black phosphorous photodetectors

Phosphorous, in its elemental nature, can exist in many forms. One such form of phosphorous is called black phosphorous (BP). With a formation energy of −395 $KJmol^{-1-}$ black phosphorous is a thermodynamically stable form of phosphorous at room temperature. Black phosphorous is similar to graphite in its appearance, properties and structure. Black phosphorous sheets have a puckered geometry [98]. Black phosphorous was first successfully exfoliated in 2014 and has received a lot of attention since then [99, 100]. In its monolayer form, the phosphorous atoms form covalent bonds with three adjacent atoms, which results in a wrinkled honeycomb structure. The corresponding layers are held together by van der Waals forces [101]. Unlike graphene, black phosphorous is a semiconductor with a direct bandgap. Due to its strong anisotropic interaction with electrons and photons, black phosphorous is a strong candidate for electronic and optoelectronic applications.

The bandgap's direct nature in black phosphorous makes it easy for the carriers to transit to excited states, as there are negligible chances of phonon scattering [102]. The

photoelectric characteristics of a black phosphorous FET were studied by Buscema et al. [103]. **Figure 4** shows the model of the device. The device operates at a wavelength ranging from visble to NIR part of the spectrum. The device shows an On/Off ratio of 10 along with an electron mobility of 0.5 $cm^2V^{-1}s^{-1}$. Wavelength ranging from visible to NIR results in a photocurrent generation in the proposed device. The responsivity exhibits a typical increase with a decreasing wavelength and attains a maximum value of 4.8 mAW^{-1}. Chen et al. used a sandwich of hBN-BP-hBN to demonstrate a photodetector with a widely tuneable infrared wavelength range [104]. The device shows an absorption of 3% at a wavelength of 3.4 μm, and the absorption of the device was observed to decrease with increasing wavelength. Furthermore, it was observed that the light absorption decreases with an increase in vertical electrical bias. Due to the vertical bias, the bandgap shrinks, giving rise to an increase in carrier concentration. The high carrier concentration results in decreased photo-carrier lifetime and degraded performance of the device. The hBN layer aims to prevent the black phosphorous from oxidation and provide a clean interface.

One of the primitive methods to improve the performance of TMDC photodetectors is to use doping. Accordingly, Keng et al. demonstrated an n-type and p-type black phosphorous photodetectors [105]. The concentration of the dopants was found to be dependent on the thickness of the black phosphorous layer. The device shows a responsivity of 1.4×10^4 AW^{-1} for a device with a black phosphorous thickness of 10 nm [105].

Using a transparent substrate opens up the possibility of novel device designs. Miao et al. have fabricated a photodetector based on multilayer black phosphorous on polyimide film substrate [106]. The device shows a responsivity of 53 AW^{-1}. It is observed that when the device is illuminated by infrared light, enhanced scattering of the carriers with the phonons occurs, which eventually degrades the carrier mobility and the performance of the device. However, such behavior is not observed when a SiO_2/Si substrate is used instead of polyimide film.

3.5 Photodetectors based on 2D-heterostructures

The ever-growing evolution and development of 2D materials have led to the formulation of 2D van der Waals heterostructures. Based on these heterostructures, several photodetectors have been reported recently. Apart from their high degree of integration, these devices exhibit excellent performance. The electronic structure and properties induced between these 2D heterostructures' layers show promising characteristics as far as electronic and optoelectronic applications are concerned. 2D heterostructures/heterojunctions are essential building blocks of modern

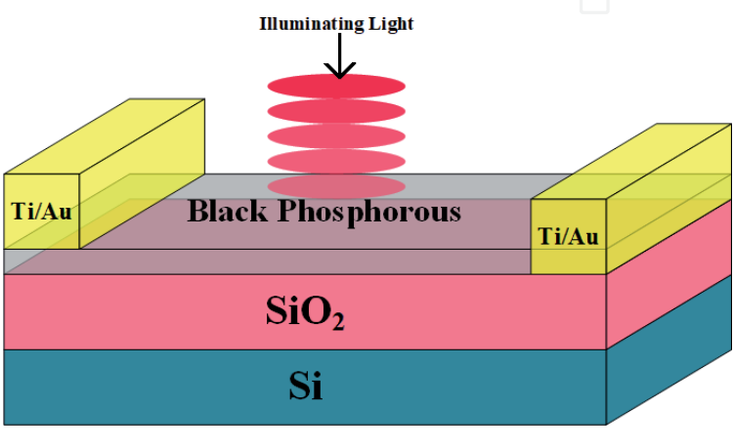

Figure 4.
Model of the few layer black phosphorous photodetector [103].

electronic devices [107]. The band structures of the constituent 2D materials of these heterostructures undergo considerable changes due to electrostatic interactions. Xue et al. have fabricated a MoS_2/WS_2 vertical heterostructures based photodetector [108]. Mo, S and WO_3 were used to prepare the MoS_2/WS_2 heterojunction. The device shows a high rectification along with a considerable responsivity of 2.3 AW^{-1}. The characteristics of the device are evaluated at an illuminatring light of 450 nm. The interfacial built-in electric field prompts the separation of the photogenerated carriers [109]. On transferring the heterojunction to the polydimethylsiloxane (PMDS) substrate, a decrease in photocurrent is observed due to trapping states between the heterojunction and the substrate [47]. Duan et al. demonstrated a heterojunction diode based on WSe_2/MoS_2 heterojunction [110]. The heterojunction was obtained by transferring the exfoliate MoS_2 to a physical vapor deposition (PVD) grown WSe_2 monolayer. A significant rectification ratio, along with high external quantum efficiency (EQE), was observed at an operating wavelength of 514 nm. It is noteworthy to mention that the EQE of the device is much higher than what is achieved in a lateral doped WSe_2 p-n homojunction [111]. Such a behavior is a consequence of the much better charge separation at the vertically stacked junction interface. Peng et al. have also reported a heterojunction between MoS_2 and WSe_2 [112]. The MoS_2/WSe_2 heterojunction is obtained by mechanical exfoliation and transfer methods. A high charge transfer of 99% from WSe_2 to MoS_2 is observed in a very short time of 470 fs [112]. The device shows promising characteristics for sub-picosecond applications.

Apart from the semiconducting materials based heterostructures, graphene has also been utilized for heterostructures formation. Graphene may not be suitable for photodetector applications independently due to its zero bandgap and high light transmittance. Yu et al. formulated a photodetector based on $MoTe_2$/graphene heterostructures [113] as shown in **Figure 5**. $MoTe_2$ multilayer serves as a light active material in the said heterostructure, and graphene monolayer serves as an efficient transport path for photo-excited carriers. The heterostructure shows better performance as compared to individual graphene and $MoTe_2$ based devices. $MoTe_2$/graphene photodetectors work on the principle of photogating effect. Due to this photogating effect, electrons are trapped in localized states of $MoTe_2$ and holes are shifted towards the graphene layer. The high carrier mobility of graphene allows for a quick extraction of the holes injected into the graphene layer. This results in an enhanced photocurrent in the device. The device shows exceptional values of photoconductive gain and responsivity.

Britnell et al. demonstrated a photodetector based on the heterostructures of a few-layer TMDCs and graphene [114]. The device's performance depends on the encapsulation of one or more layers of TMDC sheets with graphene. The device has a sandwich structure wherein the TMDC photoactive layer is encapsulated between the top and bottom graphene electrodes. Because of the transparency of graphene, the illuminating light can reach efficiently to the TMDC layer. An appreciable photocurrent is observed when the illuminating light impinges on the overlapped regions of graphene and TMDC. The direction of the photocurrent aligns with the direction of the built-in electric field resulting from the gate voltage. This allows to modulate the photocurrent through gate voltage. Due to graphene, the extraction of charges is swift, thus reducing the recombination rate of photo-excited carriers. A similar structure is reported by Duan et al. as well [115]. The device consists of a vertical sandwich of graphene-MoS_2-graphene heterojunction. Similar to the device reported by Britnell et al. [114], the top and bottom layers of graphene act as electrodes, whereas the middle MoS_2 layer acts as the barrier layer. Upon illuminating the MoS_2 layer, the electron–hole pairs get separated asymmetric potentials at the graphene/MoS_2 interface, which leads to

an appreciable photocurrent [115]. A graphene-WSe_2-graphene heterostructure based photodetector is reported by Massicotte et al. [116]. The heterostructure is packaged with hBN layers. The device exhibits an ultra-fast response time of 5.5 ps.

Apart from graphene, another novel material called silicene has received a lot of attention in recent years. Silicene, regarded as the 'silicon version of graphene,' also has a hexagonal structure [117–119]. Silicene is the single-layer version of graphene, having the constituent Si atoms arranged in a hexagonal form via covalent bonds [22, 23]. Silicene shares many properties of graphene, like zero bandgap, high mobility of carriers and the presence of a Dirac cone in its band structure. Apart from these excellent electronic properties, one advantage of silicene over graphene is its expected integration with the present state of the art Si-based technology. Kharadi et al. have proposed a photodetector based on silicene/MoS_2

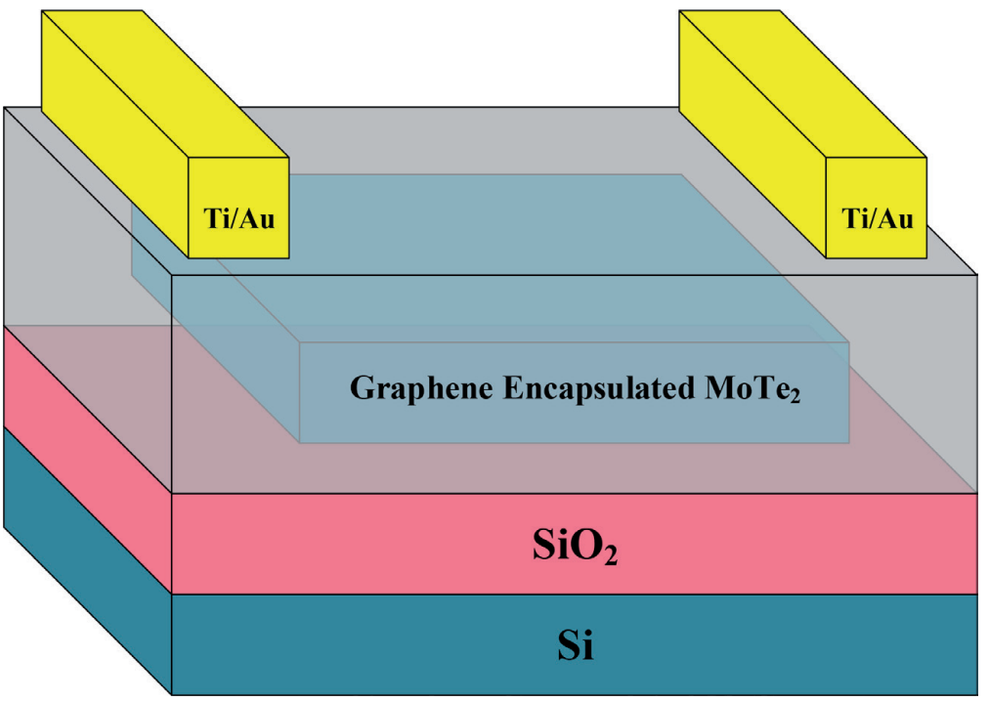

Figure 5.
Photodetector based on $MoTe_2$/graphene heterostructure [113].

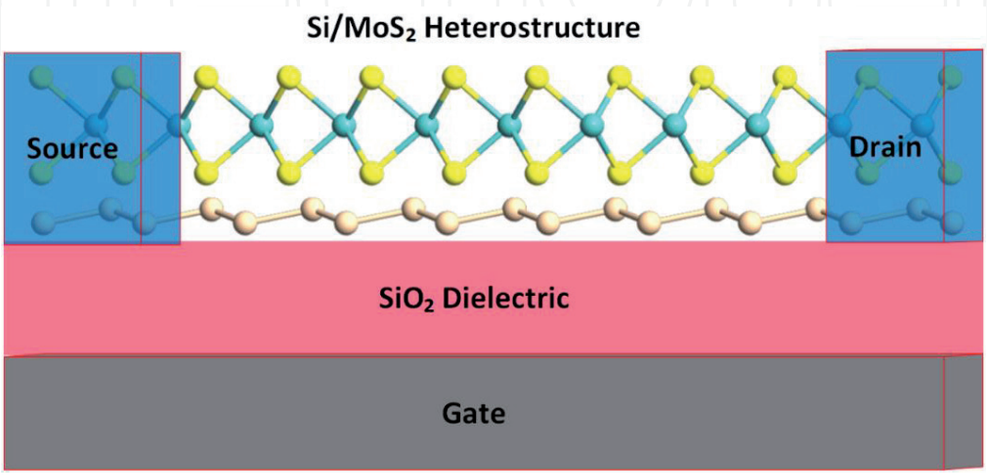

Figure 6.
Model of Si/MoS_2 heterostructure based photodetector [22].

Device Type	Wavelength	Responsivity	Response Speed	NEP/Detectivity
Single-Layer MoS_2 Phototransistor [46]	670 nm	7.5 mAW^{-1}	50 ms	—
Ultra-Sensitive Monolayer MoS_2 Photodetector [47]	680 nm	800 mAW^{-1}	0.6 s	1.5×10^{15} $WHz^{-1/2}$
High-detectivity multilayer MoS_2 phototransistors [49]	Up to NIR	100 mAW^{-1}	—	—
High-gain CVD-grown MoS_2 monolayer phototransistor [51]	532 nm	2.2×10^3 AW^{-1} in Vacuum 780 AW^{-1} in Air	—	—
High photosensitivity few-layered $MoSe_2$ back-gated field-effect phototransistor [72]	532 nm	97.1 AW^{-1}	~10 ms	—
Few Layer WS_2 Phototransistor [81]	457-647 nm	92 μAW^{-1}	5 ms	—
Multilayer WS_2 Nano-flakes Photo responsive FET [82]	633 nm	5.7 AW^{-1} in Vacuum 884 AW^{-1} in NH3 Environment	< 20 ms	—
WSe_2 Monolayer Phototransistor [84]	650 nm	1.8×10^5 AW^{-1}	< 23 ms	10^{14} Jones
High Photo responsive Few-layered WSe_2 Transistor[85]	532 nm	7 AW^{-1}	10 μs	—
$ReSe_2$ nanosheet transistor [93]	633 nm	95 AW^{-1}	~ 10 ms	—
Few-layer Black Phosphorus FET [103]	Visible-NIR	48 mAW^{-1}	—	—
Silicene/MoS_2 heterostructure [22]	650 nm	5.66×10^5 AW^{-1}	—	4.76×10^{10} Jones

Table 1.
Characteristics of photodetectors and phototransistors based on different 2D materials.

heterostructure [22]. The model of the device is shown in **Figure 6**. Due to the high mobility of carriers in silicene, it is used as a high-velocity transport path for the photo-excited carriers. Illuminating the device's active region with a light of 650 nm results in the electron–hole pair generation. The electron–hole pairs are separated at the silicene/MoS_2 heterostructure interface due to the built-in electric field generated by a combined effect of charge transfer between silicene and MoS_2 and the gate voltage. Apart from an appreciable photoconductive gain of 2.5×10^{11}, the device exhibits considerable values of responsivity (5.66×10^5 AW^{-1}) and detectivity (4.76×10^{10} Jones).

Table 1. presents the characteristics of the optoelectronic devices based on different 2D materials. In general it can be seen that the light sensitive devices based on 2D materials have shown a steady increase in the performance over the years. Depending on the bandgap of the material used, the photosensitive device can be used in different wavelength regions of the electromagnetic spectrum.

4. Summary

This chapter has summarized the present advances of the photodetectors based on 2D materials. With the ongoing research on 2D materials and their heterostructures, the class of 2D materials may mature to a large extent as far as electronic applications in general and optoelectronic applications, in particular, are concerned. Despite the promising results, certain gaps need to be bridged for the swift development of 2D material-based devices. First, convenient and cost-effective methods for the synthesis of high-quality 2D materials should be explored and developed. Second, several new properties of 2D materials are yet to be fully explored and understood. An exhaustive effort should be focused on exploring and understanding these properties. Third, more effort should be made to formulate the application-specific heterostructures of 2D materials. The electronic and optoelectronic applications may receive a heavy push upon concurrent improvements in material growth processes and fabrication methods.

The future applications of 2D materials depend on effective integration with the present Si-based technology. Materials like silicene, germanene etc., have brought a fresh breath to 2D materials' integration with Si-based technology. Though high-performance optoelectronic applications of 2D materials have been realized, there is still a lot of room for improvement. In general, one may not be surprised if wide-spread 2D material based applications are seen in the commercial market in the near future.

Author details

Mubashir A. Kharadi*, Gul Faroz A. Malik and Farooq A. Khanday
University of Kashmir, Srinagar, J&K, India

*Address all correspondence to: kharadimubashir@gmail.com

References

[1] Y. Gu, E. S. Kwak, J. L. Lensch, J. E. Allen, T. W. Odom, and L. J. Lauhon, "Near-field scanning photocurrent microscopy of a nanowire photodetector," Appl. Phys. Lett., vol. 87, no. 4, 2005, doi:10.1063/1.1996851.

[2] L. Tang *et al.*, "Nanometre-scale germanium photodetector enhanced by a near-infrared dipole antenna," Nat. Photonics, vol. 2, no. 4, pp. 226-229, 2008, doi: 10.1038/nphoton.2008.30.

[3] H. C. Liu, C. Y. Song, A. J. SpringThorpe, and J. C. Cao, "Terahertz quantum-well photodetector," Appl. Phys. Lett., vol. 84, no. 20, pp. 4068-4070, 2004, doi: 10.1063/1.1751620.

[4] J. B. K. Law and J. T. L. Thong, "Simple fabrication of a ZnO nanowire photodetector with a fast photoresponse time," Appl. Phys. Lett., vol. 88, no. 13, pp. 1-4, 2006, doi: 10.1063/1.2190459.

[5] S. Assefa, F. Xia, and Y. A. Vlasov, "Reinventing germanium avalanche photodetector for nanophotonic on-chip optical interconnects," Nature, vol. 464, no. 7285, pp. 80-84, 2010, doi: 10.1038/nature08813.

[6] H. Li, J. Wu, Z. Yin, and H. Zhang, "Preparation and applications of mechanically exfoliated single-layer and multilayer MoS2 and WSe2 nanosheets," Acc. Chem. Res., 2014, doi: 10.1021/ar4002312.

[7] M. Chhowalla, H. S. Shin, G. Eda, L. J. Li, K. P. Loh, and H. Zhang, "The chemistry of two-dimensional layered transition metal dichalcogenide nanosheets," Nature Chemistry. 2013, doi: 10.1038/nchem.1589.

[8] G. Eda, H. Yamaguchi, D. Voiry, T. Fujita, M. Chen, and M. Chhowalla, "Photoluminescence from chemically exfoliated MoS 2," Nano Lett., 2011, doi: 10.1021/nl201874w.

[9] J. N. Coleman *et al.*, "Two-dimensional nanosheets produced by liquid exfoliation of layered materials," *Science (80-.).*, 2011, doi: 10.1126/science.1194975.

[10] M. J. Allen, V. C. Tung, and R. B. Kaner, "Honeycomb carbon: A review of graphene," Chem. Rev., 2010, doi: 10.1021/cr900070d.

[11] K. S. Novoselov, V. I. Fal'Ko, L. Colombo, P. R. Gellert, M. G. Schwab, and K. Kim, "A roadmap for graphene," Nature. 2012, doi: 10.1038/nature11458.

[12] E. J. H. Lee, K. Balasubramanian, R. T. Weitz, M. Burghard, and K. Kern, "Contact and edge effects in graphene devices," Nat. Nanotechnol., 2008, doi: 10.1038/nnano.2008.172.

[13] Z. Sun and H. Chang, "Graphene and graphene-like two-dimensional materials in photodetection: Mechanisms and methodology," ACS Nano. 2014, doi: 10.1021/nn500508c.

[14] F. H. L. Koppens, T. Mueller, P. Avouris, A. C. Ferrari, M. S. Vitiello, and M. Polini, "Photodetectors based on graphene, other two-dimensional materials and hybrid systems," Nature Nanotechnology. 2014, doi: 10.1038/nnano.2014.215.

[15] J. Li, L. Niu, Z. Zheng, and F. Yan, "Photosensitive graphene transistors," *Advanced Materials*. 2014, doi: 10.1002/adma.201400349.

[16] F. Bonaccorso, Z. Sun, T. Hasan, and A. C. Ferrari, "Graphene photonics and optoelectronics," Nat. Photonics, vol. 4, no. 9, pp. 611-622, 2010, doi: 10.1038/nphoton.2010.186.

[17] F. Xia, T. Mueller, Y. M. Lin, A. Valdes-Garcia, and P. Avouris, "Ultrafast graphene photodetector,"

Nat. Nanotechnol., 2009, doi: 10.1038/nnano.2009.292.

[18] W. Bao *et al.*, "Stacking-dependent band gap and quantum transport in trilayer graphene," Nat. Phys., 2011, doi: 10.1038/NPHYS2103.

[19] A. Castellanos-Gomez, M. Poot, G. A. Steele, H. S. J. Van Der Zant, N. Agraït, and G. Rubio-Bollinger, "Elastic properties of freely suspended MoS2 nanosheets," Adv. Mater., 2012, doi: 10.1002/adma.201103965.

[20] K. He, C. Poole, K. F. Mak, and J. Shan, "Experimental demonstration of continuous electronic structure tuning via strain in atomically thin MoS2," Nano Lett., 2013, doi: 10.1021/nl4013166.

[21] H. J. Conley, B. Wang, J. I. Ziegler, R. F. Haglund, S. T. Pantelides, and K. I. Bolotin, "Bandgap engineering of strained monolayer and bilayer MoS2," Nano Lett., 2013, doi: 10.1021/nl4014748.

[22] M. A. Kharadi, G. F. A. Malik, F. A. Khanday, and K. A. Shah, "Silicene/MoS_2 Heterojunction for High-Performance Photodetector," IEEE Trans. Electron Devices, pp. 1-6, 2020, doi: 10.1109/TED.2020.3037285.

[23] M. A. Kharadi, G. F. A. Malik, K. A. Shah, and F. A. Khanday, "Performance analysis of functionalized silicene nanoribbon-based photodetector," Int. J. Numer. Model. Electron. Networks, Devices Fields, 2020, doi: 10.1002/jnm.2809.

[24] J. S. Helman and F. Sánchez-Sinencio, "Theory of Internal Photoemission," Phys. Rev. B, vol. 7, no. 8, pp. 3702-3706, Apr. 1973, doi: 10.1103/PhysRevB.7.3702.

[25] R. H. Fowler, "The Analysis of Photoelectric Sensitivity Curves for Clean Metals at Various Temperatures," Phys. Rev., vol. 38, no. 1, pp. 45-56, Jul. 1931, doi: 10.1103/PhysRev.38.45.

[26] I. Goykhman *et al.*, "On-Chip Integrated, Silicon–Graphene Plasmonic Schottky Photodetector with High Responsivity and Avalanche Photogain," Nano Lett., vol. 16, no. 5, pp. 3005-3013, May 2016, doi: 10.1021/acs.nanolett.5b05216.

[27] M. Casalino, "Silicon Photodetectors Based on Internal Photoemission Effect: The Challenge of Detecting Near-Infrared Light," L. Sirleto, Ed. Rijeka: IntechOpen, 2012, p. Ch. 3.

[28] M. Casalino, L. Sirleto, L. Moretti, and I. Rendina, "A silicon compatible resonant cavity enhanced photodetector working at 1.55 $\mathrm{\mu}$m," Semicond. Sci. Technol., vol. 23, no. 7, p. 75001, May 2008, doi: 10.1088/0268-1242/23/7/075001.

[29] R. R. Nair *et al.*, "Fine structure constant defines visual transparency of graphene," *Science (80-.).*, 2008, doi: 10.1126/science.1156965.

[30] K. F. Mak, L. Ju, F. Wang, and T. F. Heinz, "Optical spectroscopy of graphene: From the far infrared to the ultraviolet," Solid State Commun., 2012, doi: 10.1016/j.ssc.2012.04.064.

[31] T. Mueller, F. Xia, and P. Avouris, "Graphene photodetectors for high-speed optical communications," Nat. Photonics, 2010, doi: 10.1038/nphoton.2010.40.

[32] L. Zheng, L. Zhongzhu, and S. Guozhen, "Photodetectors based on two dimensional materials," J. Semicond., vol. 37, no. 9, 2016, doi: 10.1088/1674-4926/37/9/091001.

[33] T. J. Echtermeyer *et al.*, "Strong plasmonic enhancement of photovoltage in graphene," Nat. Commun., 2011, doi: 10.1038/ncomms1464.

[34] S. F. Shi, X. Xu, D. C. Ralph, and P. L. McEuen, "Plasmon resonance in individual nanogap electrodes studied using graphene nanoconstrictions as photodetectors," Nano Lett., 2011, doi: 10.1021/nl200522t.

[35] Y. Liu *et al.*, "Plasmon resonance enhanced multicolour photodetection by graphene," Nat. Commun., 2011, doi: 10.1038/ncomms1589.

[36] G. Konstantatos *et al.*, "Hybrid grapheneĝquantum dot phototransistors with ultrahigh gain," Nat. Nanotechnol., 2012, doi: 10.1038/nnano.2012.60.

[37] Z. Sun, Z. Liu, J. Li, G. A. Tai, S. P. Lau, and F. Yan, "Infrared photodetectors based on CVD-grown graphene and PbS quantum dots with ultrahigh responsivity," Adv. Mater., 2012, doi: 10.1002/adma.201202220.

[38] X. Gan *et al.*, "Chip-integrated ultrafast graphene photodetector with high responsivity," Nat. Photonics, 2013, doi: 10.1038/nphoton.2013.253.

[39] X. Wang, Z. Cheng, K. Xu, H. K. Tsang, and J.-B. Xu, "High-responsivity graphene/silicon-heterostructure waveguide photodetectors," Nat. Photonics, vol. 7, no. 11, pp. 888-891, 2013, doi: 10.1038/nphoton.2013.241.

[40] X. Zhu, W. Yan, N. A. Mortensen, and S. Xiao, "Bends and splitters in graphene nanoribbon waveguides," Opt. Express, 2013, doi: 10.1364/oe.21.003486.

[41] K. Kim, J. Y. Choi, T. Kim, S. H. Cho, and H. J. Chung, "A role for graphene in silicon-based semiconductor devices," Nature. 2011, doi: 10.1038/nature10680.

[42] N. Youngblood, Y. Anugrah, R. Ma, S. J. Koester, and M. Li, "Multifunctional graphene optical modulator and photodetector integrated on silicon waveguides," Nano Lett., 2014, doi: 10.1021/nl500712u.

[43] K. F. Mak, C. Lee, J. Hone, J. Shan, and T. F. Heinz, "Atomically Thin <math display="inline"> <msub> <mi>MoS</mi> <mn>2</mn> </msub> </math> : A New Direct-Gap Semiconductor," *Phys. Rev. Lett.*, 2010.

[44] A. Splendiani *et al.*, "Emerging photoluminescence in monolayer MoS2," Nano Lett., 2010, doi: 10.1021/nl903868w.

[45] B. Radisavljevic, A. Radenovic, J. Brivio, V. Giacometti, and A. Kis, "Single-layer MoS2 transistors," Nat. Nanotechnol., 2011, doi: 10.1038/nnano.2010.279.

[46] Z. Yin *et al.*, "Single-Layer MoS2 Phototransistors," ACS Nano, vol. 6, no. 1, pp. 74-80, Jan. 2012, doi: 10.1021/nn2024557.

[47] O. Lopez-Sanchez, D. Lembke, M. Kayci, A. Radenovic, and A. Kis, "Ultrasensitive photodetectors based on monolayer MoS 2," Nat. Nanotechnol., 2013, doi: 10.1038/nnano.2013.100.

[48] W. Jin *et al.*, "Direct measurement of the thickness-dependent electronic band structure of MoS2 using angle-resolved photoemission spectroscopy," Phys. Rev. Lett., 2013, doi: 10.1103/PhysRevLett.111.106801.

[49] W. Choi *et al.*, "High-detectivity multilayer MoS2 phototransistors with spectral response from ultraviolet to infrared," *Adv. Mater.*, vol. 24, no. 43, pp. 5832-5836, 2012, doi: 10.1002/adma.201201909.

[50] M. F. Khan, M. W. Iqbal, M. Z. Iqbal, M. A. Shehzad, Y. Seo, and J. Eom, "Photocurrent response of MoS2 field-effect transistor by deep ultraviolet light in atmospheric and N2 gas environments," ACS Appl. Mater. Interfaces, 2014, doi: 10.1021/am506716a.

[51] W. Zhang, J. K. Huang, C. H. Chen, Y. H. Chang, Y. J. Cheng, and L. J. Li,

"High-gain phototransistors based on a CVD MoS2 monolayer," Adv. Mater., 2013, doi: 10.1002/adma.201301244.

[52] C. Xie, C. Mak, X. Tao, and F. Yan, "Photodetectors Based on Two-Dimensional Layered Materials Beyond Graphene," Adv. Funct. Mater., vol. 27, no. 19, 2017, doi: 10.1002/adfm.201603886.

[53] P.-L. Néstor *et al.*, "CVD-grown monolayered MoS 2 as an effective photosensor operating at low-voltage," 2D Mater., 2014.

[54] D. S. Tsai *et al.*, "Few-layer MoS2 with high broadband photogain and fast optical switching for use in harsh environments," ACS Nano, 2013, doi: 10.1021/nn305301b.

[55] J. Li, M. M. Naiini, S. Vaziri, M. C. Lemme, and M. Östling, "Inkjet printing of MoS2," Adv. Funct. Mater., 2014, doi: 10.1002/adfm.201400984.

[56] G. Cunningham *et al.*, "Photoconductivity of solution-processed MoS2 films," *J. Mater. Chem. C*, 2013, doi: 10.1039/c3tc31402b.

[57] Z. P. Ling *et al.*, "Large-scale two-dimensional MoS_2 photodetectors by magnetron sputtering," Opt. Express, 2015, doi: 10.1364/oe.23.013580.

[58] M. M. Furchi, D. K. Polyushkin, A. Pospischil, and T. Mueller, "Mechanisms of photoconductivity in atomically thin MoS2," Nano Lett., 2014, doi: 10.1021/nl502339q.

[59] J. Lu *et al.*, "Improved photoelectrical properties of MoS2 films after laser micromachining," ACS Nano, 2014, doi: 10.1021/nn501821z.

[60] J. Kwon *et al.*, "Giant Photoamplification in Indirect-Bandgap Multilayer MoS2 Phototransistors with Local Bottom-Gate Structures," *Adv. Mater.*, 2015, doi: 10.1002/adma.201404367.

[61] D. Kufer and G. Konstantatos, "Highly Sensitive, Encapsulated MoS2 Photodetector with Gate Controllable Gain and Speed," Nano Lett., 2015, doi: 10.1021/acs.nanolett.5b02559.

[62] X. Wang *et al.*, "Ultrasensitive and Broadband MoS2 Photodetector Driven by Ferroelectrics," *Adv. Mater.*, vol. 27, no. 42, pp. 6575-6581, 2015, doi: 10.1002/adma.201503340.

[63] H. S. Lee *et al.*, "Metal Semiconductor Field-Effect Transistor with MoS2/Conducting NiO(x) van der Waals Schottky Interface for Intrinsic High Mobility and Photoswitching Speed.," ACS Nano, vol. 9, no. 8, pp. 8312-8320, Aug. 2015, doi: 10.1021/acsnano.5b02785.

[64] Y. Pang *et al.*, "Tribotronic enhanced photoresponsivity of a MOS2 phototransistor," Adv. Sci., 2015, doi: 10.1002/advs.201500419.

[65] J. D. Lin *et al.*, "Electron-doping-enhanced trion formation in monolayer molybdenum disulfide functionalized with cesium carbonate," ACS Nano, 2014, doi: 10.1021/nn501580c.

[66] D. H. Kang *et al.*, "High-Performance Transition Metal Dichalcogenide Photodetectors Enhanced by Self-Assembled Monolayer Doping," *Adv. Funct. Mater.*, 2015, doi: 10.1002/adfm.201501170.

[67] H. S. Lee *et al.*, "MoS 2 nanosheet phototransistors with thickness-modulated optical energy gap," Nano Lett., 2012, doi: 10.1021/nl301485q.

[68] Y. Zhang *et al.*, "Direct observation of the transition from indirect to direct bandgap in atomically thin epitaxial MoSe2," Nat. Nanotechnol., 2014, doi: 10.1038/nnano.2013.277.

[69] S. Tongay *et al.*, "Thermally driven crossover from indirect toward direct bandgap in 2D Semiconductors: MoSe2 versus MoS2," *Nano Lett.*, 2012, doi: 10.1021/nl302584w.

[70] J. S. Ross *et al.*, "Electrical control of neutral and charged excitons in a monolayer semiconductor," Nat. Commun., 2013, doi: 10.1038/ncomms2498.

[71] S. Larentis, B. Fallahazad, and E. Tutuc, "Field-effect transistors and intrinsic mobility in ultra-thin MoSe 2 layers," Appl. Phys. Lett., 2012, doi: 10.1063/1.4768218.

[72] A. Abderrahmane, P. J. Ko, T. V. Thu, S. Ishizawa, T. Takamura, and A. Sandhu, "High photosensitivity few-layered MoSe2 back-gated field-effect phototransistors," Nanotechnology, 2014, doi: 10.1088/0957-4484/25/36/365202.

[73] X. Lu *et al.*, "Large-area synthesis of monolayer and few-layer MoSe2 films on SiO2 substrates," Nano Lett., 2014, doi: 10.1021/nl5000906.

[74] X. Wang *et al.*, "Chemical vapor deposition growth of crystalline monolayer MoSe2," ACS Nano, 2014, doi: 10.1021/nn501175k.

[75] G. W. Shim *et al.*, "Large-area single-layer MoSe2 and its van der Waals heterostructures," ACS Nano, 2014, doi: 10.1021/nn405685j.

[76] Y. H. Chang *et al.*, "Monolayer MoSe2 grown by chemical vapor deposition for fast photodetection," ACS Nano, 2014, doi: 10.1021/nn503287m.

[77] J. Xia *et al.*, "CVD synthesis of large-area, highly crystalline MoSe2 atomic layers on diverse substrates and application to photodetectors," Nanoscale, 2014, doi: 10.1039/c4nr02311k.

[78] C. Jung *et al.*, "Highly Crystalline CVD-grown Multilayer MoSe2 Thin Film Transistor for Fast Photodetector," Sci. Rep., 2015, doi: 10.1038/srep15313.

[79] W. Sik Hwang *et al.*, "Transistors with chemically synthesized layered semiconductor WS 2 exhibiting 10 5 room temperature modulation and ambipolar behavior," Appl. Phys. Lett., 2012, doi: 10.1063/1.4732522.

[80] S. Hwan Lee, D. Lee, W. Sik Hwang, E. Hwang, D. Jena, and W. Jong Yoo, "High-performance photocurrent generation from two-dimensional WS 2 field-effect transistors," Appl. Phys. Lett., 2014, doi: 10.1063/1.4878335.

[81] N. Perea-Lõpez *et al.*, "Photosensor device based on few-layered WS2 films," *Adv. Funct. Mater.*, 2013, doi: 10.1002/adfm.201300760.

[82] N. Huo, S. Yang, Z. Wei, S. S. Li, J. B. Xia, and J. Li, "Photoresponsive and Gas Sensing Field-Effect Transistors based on Multilayer WS 2 Nanoflakes," Sci. Rep., 2014, doi: 10.1038/srep05209.

[83] C. Lan, C. Li, Y. Yin, and Y. Liu, "Large-area synthesis of monolayer WS2 and its ambient-sensitive photo-detecting performance," Nanoscale, 2015, doi: 10.1039/c5nr01205h.

[84] W. Zhang, M. H. Chiu, C. H. Chen, W. Chen, L. J. Li, and A. T. S. Wee, "Role of metal contacts in high-performance phototransistors based on WSe2 monolayers," ACS Nano, 2014, doi: 10.1021/nn503521c.

[85] N. R. Pradhan *et al.*, "High Photoresponsivity and Short Photoresponse Times in Few-Layered WSe2 Transistors," ACS Appl. Mater. Interfaces, 2015, doi: 10.1021/acsami.5b02264.

[86] J. Chen *et al.*, "Chemical Vapor Deposition of Large-Sized Hexagonal

WSe2 Crystals on Dielectric Substrates," *Adv. Mater.*, 2015, doi: 10.1002/adma.201503446.

[87] S.-H. Jo *et al.*, "A High-Performance WSe2 /h-BN Photodetector using a Triphenylphosphine (PPh3)-Based n-Doping Technique.," Adv. Mater., vol. 28, no. 24, pp. 4824-4831, Jun. 2016, doi: 10.1002/adma.201600032.

[88] Y. F. Lin *et al.*, "Ambipolar MoTe2 transistors and their applications in logic circuits," *Adv. Mater.*, 2014, doi: 10.1002/adma.201305845.

[89] C. Ruppert, O. B. Aslan, and T. F. Heinz, "Optical properties and band gap of single- and few-layer MoTe2 crystals," Nano Lett., 2014, doi: 10.1021/nl502557g.

[90] N. R. Pradhan *et al.*, "Field-effect transistors based on few-layered α-MoTe2," ACS Nano, 2014, doi: 10.1021/nn501013c.

[91] L. Yin *et al.*, "Ultrahigh sensitive MoTe2 phototransistors driven by carrier tunneling," Appl. Phys. Lett., 2016, doi: 10.1063/1.4941001.

[92] J. A. Wilson and A. D. Yoffe, "The transition metal dichalcogenides discussion and interpretation of the observed optical, electrical and structural properties," Adv. Phys., 1969, doi: 10.1080/00018736900101307.

[93] S. Yang *et al.*, "Layer-dependent electrical and optoelectronic responses of ReSe2 nanosheet transistors," Nanoscale, 2014, doi: 10.1039/c4nr01741b.

[94] S. Yang, S. Tongay, Q. Yue, Y. Li, B. Li, and F. Lu, "High-performance few-layer Mo-doped ReSe 2 nanosheet photodetectors," Sci. Rep., 2014, doi: 10.1038/srep05442.

[95] F. Liu *et al.*, "Highly Sensitive Detection of Polarized Light Using Anisotropic 2D ReS2," Adv. Funct. Mater., 2016, doi: 10.1002/adfm.201504546.

[96] S. H. Jo *et al.*, "Broad Detection Range Rhenium Diselenide Photodetector Enhanced by (3-Aminopropyl)Triethoxysilane and Triphenylphosphine Treatment," *Adv. Mater.*, 2016, doi: 10.1002/adma.201601248.

[97] J. Shim *et al.*, "High-Performance 2D Rhenium Disulfide (ReS2) Transistors and Photodetectors by Oxygen Plasma Treatment," Adv. Mater., 2016, doi: 10.1002/adma.201601002.

[98] V. V. Korolkov *et al.*, "Supramolecular networks stabilise and functionalise black phosphorus," *Nat. Commun.*, 2017, doi: 10.1038/s41467-017-01797-6.

[99] J. Miao *et al.*, "Single Pixel Black Phosphorus Photodetector for Near-Infrared Imaging," *Small*, 2018, doi: 10.1002/smll.201702082.

[100] F. Xia, H. Wang, and Y. Jia, "Rediscovering black phosphorus as an anisotropic layered material for optoelectronics and electronics," Nat. Commun., 2014, doi: 10.1038/ncomms5458.

[101] Y. Cai, G. Zhang, and Y. W. Zhang, "Layer-dependent band alignment and work function of few-layer phosphorene," Sci. Rep., 2014, doi: 10.1038/srep06677.

[102] A. N. Rudenko, S. Yuan, and M. I. Katsnelson, "Toward a realistic description of multilayer black phosphorus: From GW approximation to large-scale tight-binding simulations," *Phys. Rev. B - Condens. Matter Mater. Phys.*, 2015, doi: 10.1103/PhysRevB.92.085419.

[103] M. Buscema, D. J. Groenendijk, S. I. Blanter, G. A. Steele, H. S. J. Van

Der Zant, and A. Castellanos-Gomez, "Fast and broadband photoresponse of few-layer black phosphorus field-effect transistors," Nano Lett., 2014, doi: 10.1021/nl5008085.

[104] X. Chen *et al.*, "Widely tunable black phosphorus mid-infrared photodetector," Nat. Commun., 2017, doi: 10.1038/s41467-017-01978-3.

[105] D.-H. Kang *et al.*, "Self-Assembled Layer (SAL)-Based Doping on Black Phosphorus (BP) Transistor and Photodetector," *ACS Photonics*, vol. 4, no. 7, pp. 1822-1830, Jul. 2017, doi: 10.1021/acsphotonics.7b00398.

[106] J. Miao *et al.*, "Photothermal Effect Induced Negative Photoconductivity and High Responsivity in Flexible Black Phosphorus Transistors," ACS Nano, 2017, doi: 10.1021/acsnano.7b01999.

[107] S. J. Haigh *et al.*, "Cross-sectional imaging of individual layers and buried interfaces of graphene-based heterostructures and superlattices," Nat. Mater., 2012, doi: 10.1038/nmat3386.

[108] Y. Xue *et al.*, "Scalable Production of a Few-Layer MoS2/WS2 Vertical Heterojunction Array and Its Application for Photodetectors.," ACS Nano, vol. 10, no. 1, pp. 573-580, Jan. 2016, doi: 10.1021/acsnano.5b05596.

[109] X. Hong *et al.*, "Ultrafast charge transfer in atomically thin MoS2/WS2 heterostructures," Nat. Nanotechnol., vol. 9, no. 9, pp. 682-686, 2014, doi: 10.1038/nnano.2014.167.

[110] R. Cheng *et al.*, "Electroluminescence and photocurrent generation from atomically sharp WSe2/MoS2 heterojunction p-n diodes.," Nano Lett., vol. 14, no. 10, pp. 5590-5597, Oct. 2014, doi: 10.1021/nl502075n.

[111] A. Pospischil, M. M. Furchi, and T. Mueller, "Solar-energy conversion and light emission in an atomic monolayer p-n diode," Nat. Nanotechnol., 2014, doi: 10.1038/nnano.2014.14.

[112] B. Peng *et al.*, "Ultrafast charge transfer in {MoS} 2 /{WSe} 2 p{\ textendash}n Heterojunction," *2D Mater.*, vol. 3, no. 2, p. 25020, May 2016, doi: 10.1088/2053-1583/3/2/025020.

[113] W. Yu *et al.*, "Near-Infrared Photodetectors Based on MoTe2/Graphene Heterostructure with High Responsivity and Flexibility," Small, vol. 13, no. 24, p. 1700268, 2017, doi: https://doi.org/10.1002/smll.201700268.

[114] L. Britnell *et al.*, "Strong light-matter interactions in heterostructures of atomically thin films," *Science (80-.).*, 2013, doi: 10.1126/science.1235547.

[115] W. J. Yu *et al.*, "Highly efficient gate-tunable photocurrent generation in vertical heterostructures of layered materials," Nat. Nanotechnol., 2013, doi: 10.1038/nnano.2013.219.

[116] M. Massicotte *et al.*, "Picosecond photoresponse in van der Waals heterostructures," Nat. Nanotechnol., 2016, doi: 10.1038/nnano.2015.227.

[117] M. A. Kharadi, G. F. A. Malik, F. A. KHANDAY, K. Shah, S. Mittal, and B. K. Kaushik, "Review—Silicene: From Material to Device Applications," ECS J. Solid State Sci. Technol., Dec. 2020, doi: 10.1149/2162-8777/abd09a.

[118] M. A. Kharadi, G. F. A. Malik, K. A. Shah, and F. A. Khanday, "Sub-10-nm Silicene Nanoribbon Field Effect Transistor," IEEE Trans. Electron Devices, 2019, doi: 10.1109/TED.2019.2942396.

[119] M. A. Kharadi, G. F. A. Malik, F. A. Khanday, and K. A. Shah, "Hydrogenated silicene based magnetic junction with improved tunneling magnetoresistance and spin-filtering efficiency," Phys. Lett. A, vol. 384, no. 32, p. 126826, 2020, doi: https://doi.org/10.1016/j.physleta.2020.126826.